

ICA APPLICATION FOR CBIR

Arti Khaparde^{1,2}, B.L.Deekshatulu², M.Madhavilatha³

¹Electronics and Telecommunication, ATRI, Hyderabad, India

²Computer & Information Science, HCU, Hyderabad, India

³Electronics and Telecommunication, JNTU Hyderabad, India

Corresponding Author's E-mail: artikhaparde@gmail.com

Abstract— Content Based Image Retrieval (CBIR) has become one of the most active research areas in the past few years. Many indexing techniques are based on global features distribution such as Gabor Wavelets. In this paper we present a new approach for global feature extraction using an emerging technique known as Independent Component Analysis (ICA). ICA is a generative model for observed multivariate data, which are assumed to be mixtures of some unknown latent variables. It is a statistical and computational technique for revealing hidden factors that underlies set of random variable measurements of signals. The objective of ICA is to represent a set of multidimensional measurement vectors in a basis where the components are statistically independent. Present papers deals with the comparative study between ICA feature vectors and Gabor feature vectors for 180 different texture and natural images in a databank. Result analysis show that extracting color and texture information by ICA provides significantly improved results in terms of retrieval accuracy, computational complexity and storage space of feature vectors as compared to Gabor approaches.

1 INTRODUCTION

Recent years have witnessed a rapid increase of the volume of digital image collection, which motivates the research of CBIR. To avoid manual annotation many alternative approaches were introduced by which images would be indexed by their visual content such as color, texture, shape etc. Many research efforts have been made to extract these low level image features, evaluate distance metrics and look for efficient searching schemes.

A CBIR is a two step approach to search the image in database. First, for each image in the database, a feature vector is computed and stored in feature database. Second given a query image, its feature vector is compared to the feature vectors in the data base and images most similar to the query image are returned to the user. The feature and similarity measure used to compare two feature vectors should be efficient enough to match similar images.

We have presented ICA of images as a computational technique for creating a new data dependent filter bank. The new ICA filter bank is similar to the Gabor filter bank but it

seems to be richer in the sense that some filters have more complex frequency responses. They are able to capture the inherent properties of textured images. The ICA based approach is different from existing filtering methods in that it produces a data dependent filter bank.

This paper describes an image retrieval technique based on ICA and the results are compared with the Gabor features. We demonstrate our retrieval results both for texture images and for natural images.

The paper is organized as follows : Section 2 describes fundamentals of 2-D Gabor filters. Section 3 describes ICA. Section 4 discusses ICA algorithm for separation of mixed images. In section 5, we present experimental results for separation of mixed images, response of ICA for an individual image and image retrieval based on Gabor as well as ICA feature vector. Section 6 concludes the paper with future scope.

2. GABOR FILTER WAVELETS

Gabor wavelet is widely adopted to extract texture features from the images for retrieval and has been shown to be very efficient. Basically Gabor filters are a group of wavelets, with each wavelet capturing energy at a specific frequency and specific orientation. The scale and orientation tunable property of Gabor filter makes it especially useful for texture analysis. The design of Gabor filter is done as follows: [Clause 2000, Zhang 2003]

For a given image $I(x,y)$ with size $P \times Q$, its discrete Gabor wavelet transform is given by a convolution:

$$G_{mn}(x, y) = \sum_s \sum_t I(x-s, y-t) \psi_{mn}^*(s, t) \quad (1)$$

where, s and t are the filter mask size variables, and ψ_{mn}^* is a complex conjugate of ψ_{mn} which is a class of self-similar functions generated from dilation and rotation of the following mother wavelet:

$$\psi(x, y) = \frac{1}{2\pi\sigma_x\sigma_y} \exp\left[-\frac{1}{2}\left(\frac{x^2}{\sigma_x^2} + \frac{y^2}{\sigma_y^2}\right)\right] \cdot \exp(j2\pi Wx) \quad (2)$$

where W is called the modulation frequency. The self-similar Gabor wavelets are obtained through the generating function:

$$\psi_{mn}(x, y) = a^{-m} \psi(\tilde{x}, \tilde{y}) \quad (3)$$

where m and n specify the scale and orientation of the wavelet respectively, with $m=0,1,\dots,M-1$, $n=0,1,\dots,N-1$, and

$$\begin{aligned}\tilde{x} &= a^{-m}(x \cos \theta + y \sin \theta) \\ \tilde{y} &= a^{-m}(-x \sin \theta + y \cos \theta)\end{aligned}\quad (4)$$

where $a > 1$ and $\theta = n\pi / N$.

The variables in the above equation are defined as follows:

$$\begin{aligned}a &= (U_h / U_l)^{\frac{1}{M-1}}, \\ W_{m,n} &= a^m U_l\end{aligned}\quad (5)$$

$$\begin{aligned}\sigma_{x,m,n} &= \frac{(a+1)\sqrt{2\ln 2}}{2\pi a^m (a-1)U_l}, \\ \sigma_{y,m,n} &= \frac{1}{2\pi \tan(\frac{\pi}{2N}) \sqrt{\frac{U_h^2}{2\ln 2} - (\frac{1}{2\pi\sigma_{x,m,n}})^2}}\end{aligned}\quad (6)$$

In our implementation, we used the following constants as commonly used in the literature:

$U_l=0.05$, $U_h=0.4$, s and t range from 0 to 60, i.e., filter mask size is 60x60.

3. INDEPENDENT COMPONENT ANALYSIS

Independent Component Analysis is a method for finding underlying factors or components from multivariate data. The approach that distinguishes ICA from other methods is that it looks for components that are both statistically independent and non-Gaussian.

ICA of known random vector \mathbf{X} consists of estimating the following generative model for the data

$$\mathbf{X} = \mathbf{A}\mathbf{S} \quad (7)$$

where \mathbf{X} is the mixed matrix, \mathbf{A} is the mixing matrix, \mathbf{S} is the source matrix, such that the components S_i (source signals) are as independent as possible, with respect to some maximum function that measures independence

The properties of the ICA method depend on both of the objective function and the optimization algorithm. In particular the statistical properties depend on the choice of the objective function whereas the algorithm depends on the optimization function.

One of the simple and intuitive principle for estimating the model of ICA is based on

maximization of non-gaussianity. Non-gaussianity is actually of paramount importance in ICA estimation. Without non gaussianity the estimation is not possible at all [1]. Therefore it is not surprising that non gaussianity could be used as a leading principle in ICA estimation. The present work mainly deals with the above algorithm studied from the references [Hyvarien 1997,1999, 2000,Comon 1994] and applied to different applications.

The following algorithm motivates the maximization of non-Gaussianity by the central limit theorem. As a first practical measure of non-Gaussianity, fourth order cumulant or kurtosis is explained in section 3.1.1. In the section 3.1.2 the information theoretic quantity called negentropy, as an alternative measure of non-Gaussianity is also introduced and explained briefly. The original FastICA algorithm as given by Appo Hyvarien(1999) is modified and applied to images, which is explained in section 4.

3.1 Measures of Non-Gaussianity

3.1.1 Kurtosis. To use non-gaussianity in ICA, one must have a quantitative measure of non-Gaussianity of random variable. In literature it has been proved that High order contrast function (eg: Kurtosis) can be used for ICA. The classical measure of non-gaussianity is kurtosis or the fourth order cumulant. It is defined by

$$kurt(y) = E\{y^4\} - 3\left(E\{y^2\}\right)^2 \quad (8)$$

As the variable y is assumed to be standardized i.e. zero mean and unit variance we can say

$$kurt(y) = E\{y^4\} - 3 \quad (9)$$

Hence the kurtosis is simply a normalized version of the fourth moment $E\{y^4\}$. For the Gaussian case the fourth moment is equal to $3\left(E\{y^2\}\right)^2$ and hence $kurt(y) = 0$. Thus for Gaussian variable kurtosis is zero but for most non-gaussian random variable it is non-zero.

Let us consider that y is one of ICs given as

$$y = b^T X = b^T AS = q^T S = q_1 s_1 + q_2 s_2 \quad (10)$$

where b is the estimated value. Therefore

$$Kurt(y) = q_1^4 Kurt(s_1) + q_2^4 Kurt(s_2) \quad (11)$$

The constraint is that the variance of y is equal to 1, which implies that

$$E\{y^2\} = q_1^2 + q_2^2 = 1 \quad (12)$$

Geometrically, this means that vector q is constrained to be the unit circle on the 2-D plane.

The optimization problem is now to find the maxima of the function

$$|kurt(y)| = |q_1^4 kurt(s_1) + q_2^4 kurt(s_2)| \quad (13)$$

on the unit circle. Let for simplicity assume that kurtosis is equal to 1. Hence from equation 13, we can say

$$F(q) = q_1^4 + q_2^4 \quad (14)$$

Some contours of this function are shown on Figure below, where the thick curve is the unit sphere, and the thin curves are the contours where the above function is constant.

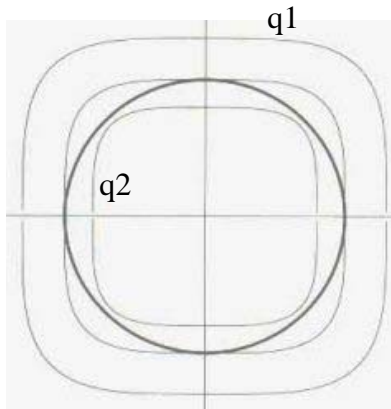


Figure 1. The optimization landscape of kurtosis

It is not hard to show (Delfasse and Loubaton, 1995) that the maxima are at the points when exactly one of the element vectors of q is zero and the other non-zero, because of the unit circle constraint, the non zero element must be equal to 1 or -1 . But these points are exactly the ones when y equals one of the independent components of S , and therefore the problem has been solved.

In general if the kurtoses are completely arbitrary, as long as they are non-zero, more involved algebraic manipulations shows that the absolute value of kurtosis is still maximized when $y = b^T X$ equal to one of ICs. The plot of convergence of ICA(Figure 8) in given results proves the above concept.

3.1.2 Negentropy. Negentropy is another very important measure of non-gaussianity. To obtain a measure of non-gaussianity that is zero for a gaussian variable and always non negative for a random variable, a slightly modified version of the definition of differential entropy called negentropy can be used.

Negentropy J is defined as

$$J(y) = H(Y_{gauss}) - H(y) \quad (15)$$

where Y_{gauss} is a gaussian random variable of the same covariance matrix as y .

As the gaussian variable has the largest entropy among all the random variables, the negentropy for the random variables will always be positive and it is zero if and only if it is a gaussian variable. Moreover, the negentropy has an additional property that it is invariant for invertible transformation.

But the estimation of negentropy is difficult, as it would require an estimate of the pdf. Therefore in practice negentropy is approximated by using higher order moments.

$$J(y) \approx \frac{1}{12} E\{y^3\}^2 + \frac{1}{48} \text{kurt}(y)^2 \quad (16)$$

Again the random variable y is assumed to be standardized i.e. zero mean and unit variance.

In order to increase the robustness another approach is to generalize the higher order cumulant approximation, so that it uses expectations of general non-quadratic functions. As a simple case, consider any two non-quadratic functions G_1 and G_2 so that G_1 is odd and G_2 is even and the following approximation is obtained.

$$J(y) \cong K_1 \left(E\{G_1(y)\} \right)^2 + K_2 \left\{ E\{G_2(y)\} - E\{G_2(U)\} \right\}^2 \quad (17)$$

where K_1 and K_2 are positive constant and U is standardized gaussian variable.

The non-quadratic function G should be chosen such that it does not grow too fast. It will help to obtain more robust estimator. In literature the following choices of G have proved very useful –

$$G = \tanh(y)$$

$$G = y^3$$

$$G = -\exp\left(-\frac{y^2}{2}\right)$$

$$G = \frac{1}{a} \log \left\{ \cosh(ay) \right\} \quad (18)$$

For the present work, the first two non-linearities have been used.

Thus this approximation gives a very good compromise between the properties of two classic non-gaussianity measures – Kurtosis and negentropy. They are conceptually simple, fast to compute and robust. And therefore can be used as objective function in ICA method.

4. ICA ALGORITHM

The use of kurtosis can lead to a much faster method for maximizing negentropy as compared to the present day gradient methods. It is introduced as fixed point algorithm in

the literature, by Appo Hyvarien and E.Ojha, for 1-D signals. This algorithm finds a direction for a unit vector W such that the projection $W^T Z$ maximizes non-gaussianity. Non gaussianity is measured by the approximation of negentropy $J(W^T Z)$, where the variance of $W^T Z$ must be constrained to unity. For whitened data this is equivalent to constraining the norm of W to be unity.

FastICA is based on a fixed point iteration scheme for finding a maximum of the non gaussianity of $W^T Z$. It can be derived as an approximative Newton iteration. The FastICA algorithm using negentropy combines the superior algorithmic properties resulting from the fixed point iteration with the preferable statistical properties due to negentropy. The FastICA algorithm stated by Aapo Hyvarinen and E.Oja was modified because during the course of the work it was observed that if the Principle Component Analysis (PCA) is done first and then whitening, then not only the computational complexity reduces but it greatly reduces the time taken by the algorithm to converges, especially for the image data. Therefore the modified and applied FastICA algorithm is as follows:

1. Center the given data X to make its mean zero.
2. Choose m , the number of independent components to estimate from the PCA.
3. Whiten the output data to give Z .
4. Choose the random mixing matrix W
5. Orthogonalized the matrix W
6. Let

$$W_1 \leftarrow E \left\{ Z g \left(W^T Z \right) \right\} - E \left\{ g' \left(W^T Z \right) \right\} W$$

where g is defined as

$$g(y) = \tanh(y) \text{ or } \\ g(y) = y^3$$

7. Orthogonalized matrix W
8. Let

$$W_2 \leftarrow \frac{W_1}{\|W_1\|}$$

9. If not converged, go back to step 6.
10. For next IC go to step 6, repeat till all ICs are estimated

Here convergence means that the old and new value of W point in the same direction i.e., the absolute value of their dot product is (almost) equal to 1.

5. EXPERIMENTAL RESULTS

5.1 For Separation of Mixed Images

The following is the set of three images that were used to find the mixed image, Figure 4, which was given as an input to algorithm.

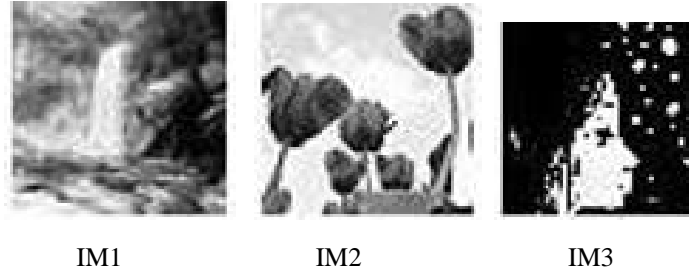


Figure 2. Reference Input Images

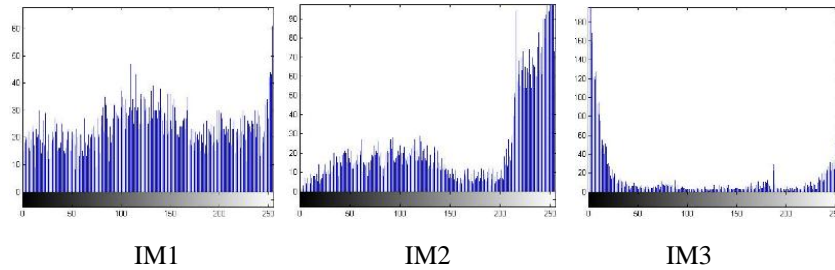


Figure 3. Histogram of above images

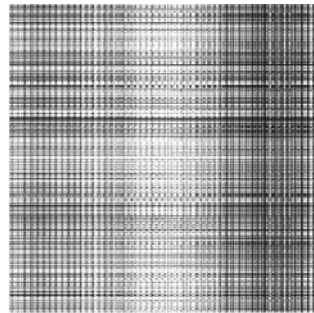


Figure 4. Mixed Image

Figure 5 is a scatter plots of the columns of X against the columns of Y. and the diagonal is histogram of $Y(:,i)$, Here it can be observed that the number of PCA having value above the threshold, $1e-7$ (from literature/internet), is equal to three, which is equal to number of images considered to get mixed matrix.

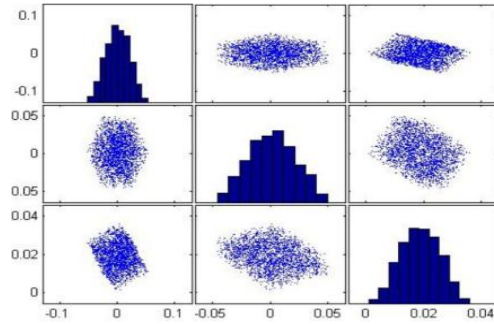


Figure 5. PCA Output

Figure 6 gives the plot of whitened matrix where the given data is made as independent as possible. In this case every column is made independent with respect to column 1.

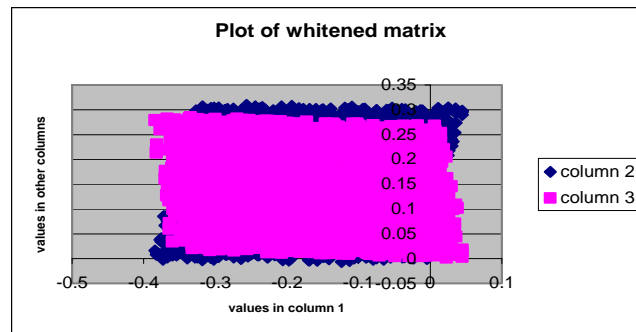


Figure 6. Whitened Matrix

Figure 7 gives the plot for ICA. It can be observed that All ICs are in the same direction as mention in section 4.

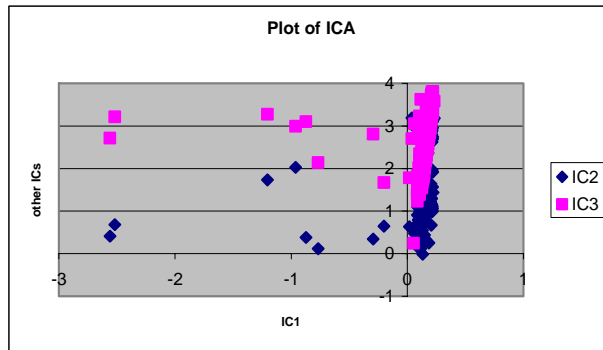


Figure 7. ICA Plot

Figure 8 proves that the algorithm converges when the values lies between some \pm constant values as explained in section3.1.1. Here it is ± 0.0075 and ± 0.01 approx.

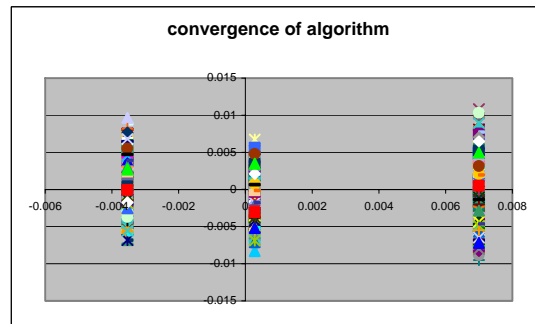


Figure 8. Plot for Convergence of ICA Algorithm

Figure 9 gives the plot for dewhitened matrix. Here the maximum values of the matrix lie in first and fourth quadrant. Hence atleast one of the retrieved images may be negative of IM1, IM2 or IM3.(Conclusion done on the basis of the simulation results for many set of mixed images)

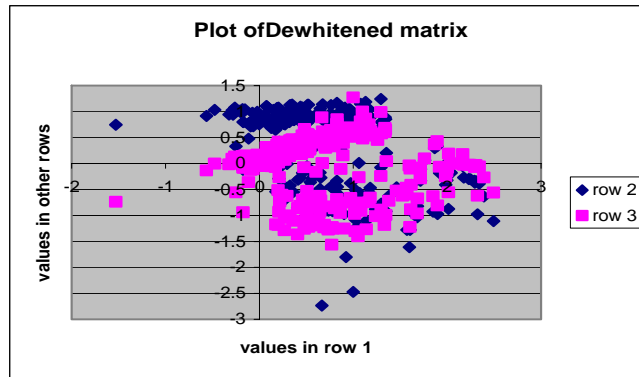


Figure 9 Dewhitened Matrix

From Figure10, it can be observed that the third image is the negative image of IM3.

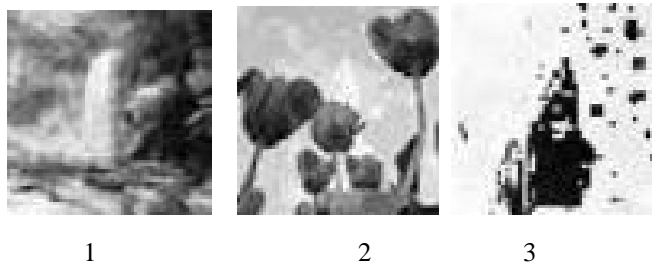


Figure 10 Retrieved images

5.2 ICA Response

ICA is a very general-purpose statistical technique in which observed random data are linearly transformed into components that are maximally independent from each other, and simultaneously have interesting distributions. The above algorithm was implemented on the image data and the Figure 11 shown below gives the plot of Independent Components for two different images, flag and pebbles respectively, which were used as query image for CBIR.

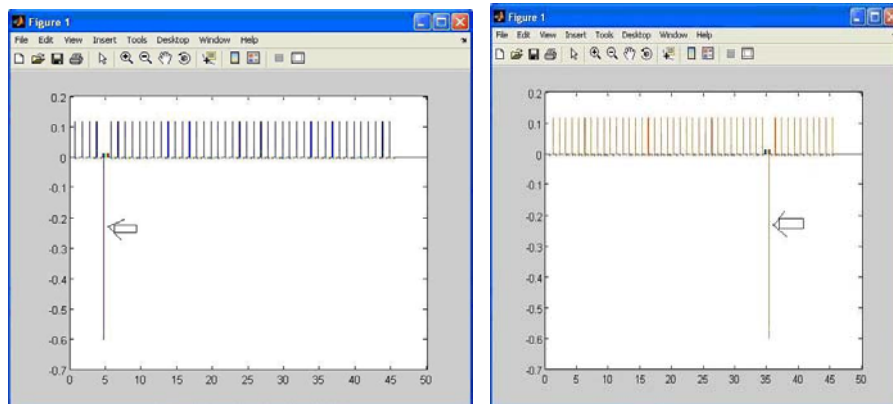


Figure 11 Response of Independent Components of two different Images

The plot shows the kurtosis, marked as \Leftarrow , is always negative, and is minimized in the directions of the independent components. These correspond to the direction in which the absolute value of the kurtosis is maximized. Thus, these independent components give a unique identity to every image, thereby achieving local maxima at different points. Initially, the ICA algorithm was developed for separating the mixed 1-D signals but considering the above response for single image along with the concept that the IC of natural scenes are edge filters[8] it was used to find the features for CBIR.

5.3 Experimental Results for CBIR

We design a Gabor wavelet for 5 scales and 6 orientations. We have conducted retrieval test both on texture images and natural images. The data is composed of 18 different kind of images such as tulip, texture, satellite image, animal, airplane, flag, natural images etc. There are 10 images of every kind which means there are total 180 images in a databank.

The retrieve results are shown in figures [12-14] are for the flag as the query image and that shown in figures [15-17] are for pebbles as the query image. The first 32 retrieve images using ICA and Gabor are shown in. The retrieve images are ranked in the decreasing order based on the similarity of their features to those of the query image.

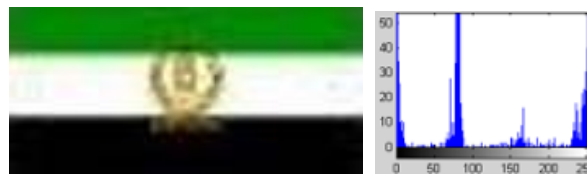


Figure 12. Flag as Query and its histogram

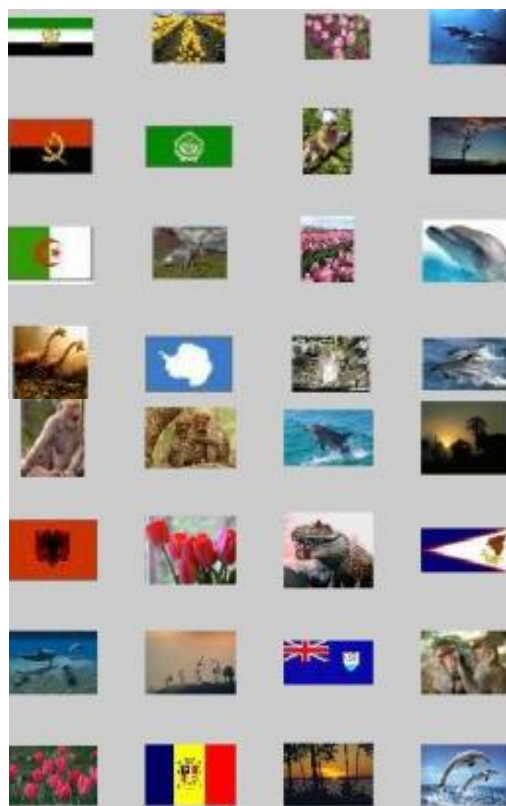


Figure13. Retrieved images using ICA for Flag (query)



Figure 14. Retrieved images using Gabor for Flag (query)

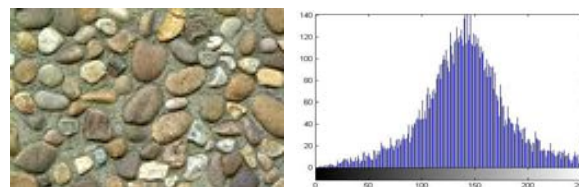


Figure 15. Pebbles texture and its histogram.



Figure 16. Retrieved images using ICA for Pebble (query)

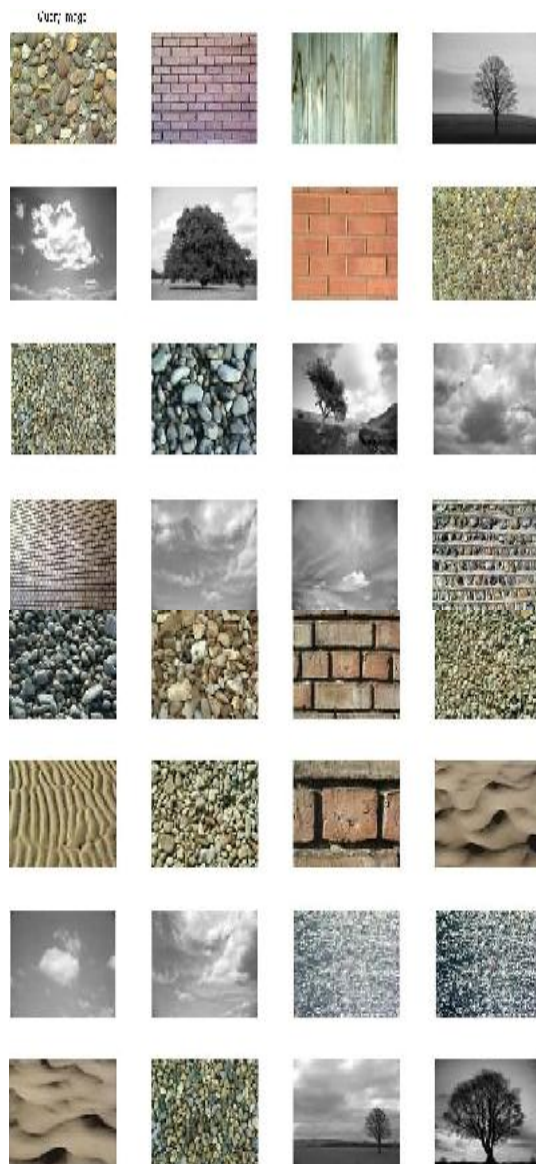


Figure 17. Retrieved images using Gabor for Pebble (query)

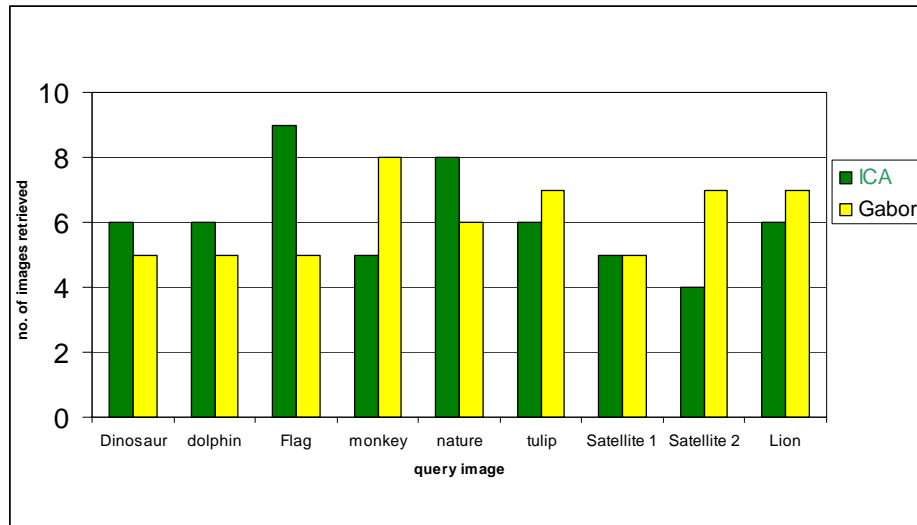


Figure 18(a). Comparative analysis for the retrieval efficiency for 9 different query images

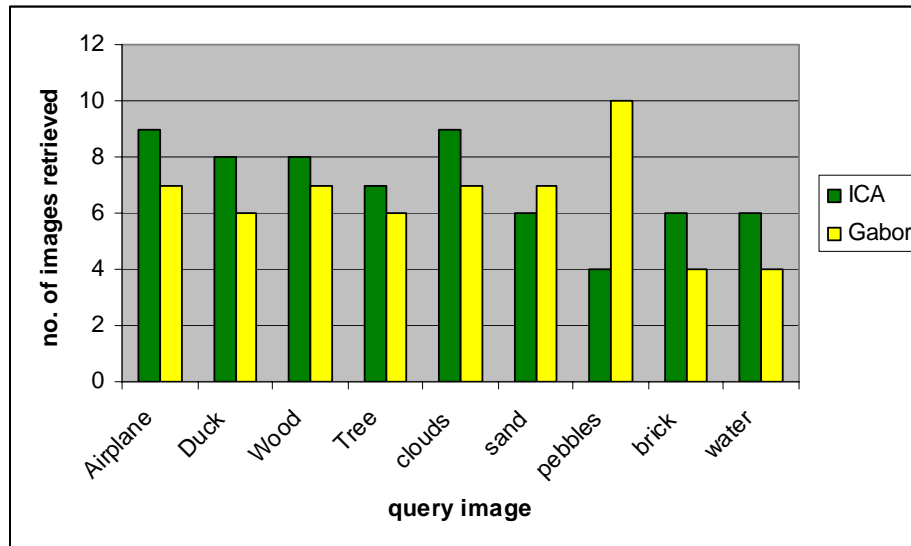


Figure 18(b). Comparative analysis for the retrieval efficiency for 9 different query images

Figure 18(a) and Figure 18(b) shows the comparative analysis for retrieval efficiency for all the 18 queries. For illustration we provide the 2 query images along with their histograms, where we found some interesting results with respect to their histogram. If we compare the analysis of the retrieval efficiency with the histogram of the query image it can be seen that the histogram which is having a single peak with nearly Gaussian distribution can be retrieve very efficiently by Gabor filters (Figure 15), whereas the histogram which is having two or more peaks can be retrieve very efficiently using ICA filters (Figure 12.). We found that these results are mostly true for other query images also.

6. CONCLUSION AND FUTURE SCOPE

The FastICA algorithm was applied to mixed image. It was also applied to CBIR. The results of CBIR using ICA are then compared with CBIR using Gabor wavelets. The consolidated summary of the conclusions for mixed image separation and Content Based Image Retrieval can be stated as follows:

The number of images mixed can be understood by seeing at PCA output. The number of PCA will give the number of images that are mixed in the given input mixed matrix. Whitening is difficult if the number of images mixed is increased and hence the chance of getting the overlapped images also increases. But still images are readable

which proves that ICA is stronger than whitening. Depending of dewhitening matrix the image is obtained. If the maximum number of dewhiteneing coefficient lies in second and/or fourth quadrant, then original image is retrieved otherwise image retrieved is negative.

The new ICA filter bank is similar to the Gabor filter bank, but it seems to be richer in the sense that some filters have more complex frequency responses. For the retrieval of the images having non Gaussian distribution of the gray scales, ICA works far better than Gabor wavelets while for the images having near about Gaussian distribution of gray scales Gabor works better than ICA. Except for certain distribution of pixels with gray scale, where either ICA or Gabor works very well, experiments using multi-textured images shows that the ICA filter bank yield similar or better results than the Gabor Filter bank. Also, in the case of Gabor analysis, global texture features are extracted from the entire image; the extracted texture features are then used to measure the similarity between images. This method is most useful if the entire image or main part of the image has a uniform texture. In reality, an image may be considered as a mosaic of different texture regions. ICA can be of help in case of images with non-uniform texture. It was also observed that memory require to store the ICA features is too less as compared to the Gabor features which can be an additional advantage in order to increase the retrieval speed.

The present work deals with the FastICA algorithm for Images and CBIR. As in literature FastICA has been proved best for the 1-D signals, it was extended for the images. The present work can be extended by applying the other ICA algorithms and a comparative study can be performed.

During the course of the work, implementation of PAST (Projection Approximation Subspace Tracking) algorithm was also tried on the images. As a future scope it can be considered as the upcoming algorithm, as it was observed that time taken to converge that algorithm was less. The only drawback which was observed was that the retrieved images were highly overlapped, which may be removed by considering more stringent convergence criteria.

The present work just introduces the concept, that ICA can be implemented for CBIR. It can give the better results than Gabor filter if the distribution of gray scales are non-Gaussian. Hence it can be further extended by applying the preprocessing steps as those applied to the present CBIR techniques.

REFERENCES

1. A. HYVARINEN, 1999, Survey of independent component analysis. *Neural Computing Surveys*, **2**, pp. 94-128.
2. A. HYVARINEN AND E. OJA, 2000, Independent component analysis: Algorithms and application. *Neural Networks*, **13**, pp. 411-430.
3. A. HYVARINEN, 1999, Fast and robust fixed-point algorithms for independent component analysis. *IEEE Trans. on Neural Networks*, **10(3)**, pp. 626-634.

4. A. HYVARINEN AND E. OJA, 1997 A fast fixed-point algorithm for independent component analysis. *Neural Computation*, **9(7)**, pp. 1483-1492.
5. ARTI KHAPARDE, M.MADHAVILATHA, 2006, Iris Recognition using Gabor filters and xeta square statistics, *Proceeding of IFToMM-PCEA International conference PICA-July 2006*, Nagpur, India.
6. ARTI KHAPARDE, M MADHAVI LATHA, M.B.L. MANASA, S.PRADEEP KUMAR, P. ANIL BABU,2008, Mixed Image Separation Using Fast ICA, *A reference of series book New Aspects of Signal Processing and wavelets*, published by WSEAS press, pp. 145-152.
7. ARTI KHAPARDE, B.L.DEESHATULU, M.MADHAVI LATHA, ZKIRA FARHEEN SANDHYA KUMARI V, 2008, Content Based Image Retrieval Using Independent Component Analysis, *International Journal of Computer Science and Netwrok Security*, **8(4)**, pp. 327-332.
8. A.J.BELL AND T.J.SEJNOWSKI,1997, The ‘independent components’ of natural scenes are edge filters. *Vision Research*, **37**, pp. 3327-3338.
9. DAVID A CLAUSE, M.ED JERNIGAN, 2000 Designing Gabor filters for optimal texture separability, *Pattern Recognition*, **33**, pp.1835—1849.
10. DENGSHENG ZHANG, AYLWIN WONG, MARIA INDRAWAN, AND GUOJUN LU, 2003, Content Based Image Retrieval using Gabor Texture features, available online, Australia.
11. MANTHALAKAR R, .BISWAS P.K, CHATTERJI B. N, 2003, Rotation and scale invariant texture features using discrete wavelet packed transform. *Pattern Recognition letter* **24(14)**, pp. 2455—2462.
12. P. COMON, 1994, Independent component analysis—a new concept? *Signal Processing*, **36**, pp. 287-314.